Sumerianz Journal of Scientific Research, 2022, Vol. 5, No. 2, pp. 44-52
ISSN(e): 2617-6955, ISSN(p): 2617-765X
Website: https://www.sumerianz.com
DOI: https://doi.org/10.47752/sjsr.52.44.52

Original Article Open Access

Hazard Flood Mapping and Monitoring in Parts of the Niger Delta Region Using Sentinel 1 Synthetic Aperture Radar

Eteh Desmond Rowland *
Niger Delta University, Wilberforce Island, Amassoma. Bayelsa State, Nigeria
Email: desmondeteh@gmail.com

Ebiegberi Oborie
Niger Delta University, Wilberforce Island, Amassoma. Bayelsa State, Nigeria
Email: desmondeteh@gmail.com

*(Corresponding author)

Article History

Received: 3 March 2022

Revised: 25 April 2022

Accepted: 10 May 2022

Published: 15 May 2022

How to Cite

Eteh, D. R.., and Ebiegberi, O., 2022. "Hazard Flood Mapping and Monitory in Parts of the Niger Delta Region Using Sentinel 1 Synthetic Aperture Radar." *Sumerianz Journal of Scientific Research*, vol. 5, pp. 44-51.

Abstract

In this study, the RGB band and threshold techniques were used to distinguish between the flooded area and permanent water bodies with the use of Sentinel 1 images to map and monitor flood hazards in Yenagoa, Bayelsa State. The acquired images were before the flood events in January 2019 and during the events in October and November 2019 with the aid of Snap 7.0 and ArcGIS software. The preprocessing of Sentinel-1 images and the mapping procedure have been described in detail, and the results have been evaluated. The results show that the Sentinel 1 sensor can rapidly provide quality data in mapping floods. The applied techniques, RGB and Threshold, show a clear disparity between permanent water bodies and floods by applying contact stretch to histograms. Zones with low backscatter signify flooded areas in red, with high radar response signifying land in the archive indicating surfaces. Areas with black indicate permanent waterbodies, while areas with white indicate built up areas. The estimated significant difference in mean water surface for January and October 2019 is -0.23 dB, while for January and November 2019 it is-0.36 decibels (dB). The difference between October and November 2019 is -0.12 decibels (dB) for the estimated mean water surface in the study area. Therefore, emphasizing remote sensing and GIS as essential tools for flood mapping, risk analysis, and better flood management is therefore essential.

Keywords: Remote sensing; Sentinel 1; Flood; Backscatter; Contact stretch; RGB; Threshold.

1. Introduction

Flooding is a major global issue that affects both developed and developing countries. It has displaced many people and destroyed farms and infrastructure. Recent examples include floods in Yenagoa, Amassoma, and other parts of Bayelsa State in 2012, 2018, and 2019 [1]. Floods have been a major hydrological and environmental problem in Nigeria, particularly in the Niger Delta Region, over the last decade. This phenomenon is widely thought to be a result of global climate change on our planet, and it is exacerbated by anthropogenic factors such as deforestation, poor urban planning, and blocked drainage. Flooding has harmed many aspects of the region's economy, including the destruction of farms and infrastructure, resulting in a food crisis and an increase in poverty. Another peculiar challenge that flooding presents in the study area is that groundwater, which is the primary source of drinking water, is highly susceptible to contamination from percolating flood waters because the water table is very close to the surface and the majority of private water boreholes in the study area are shallow (generally 50m). Floods are also to blame for facilitating the transportation and spread of pollutants from indiscriminate open dump-sites, which are common in parts of the study area. According to the United Nations Office for Disaster Risk Reduction (UNISDR) in The United Nations Office for Disaster Risk Reduction UNISDR [2] many countries consider uncontrolled storm water to be their most serious problem when it comes to the preservation of urban infrastructure. Many neighborhoods in Bangkok, Calcutta, Dar es Salaam, Jakarta, Guayanguil, Manila, and Lagos

are flooded at least once a year, and residents live with the water in their homes [3, 4]. SAR (Synthetic Aperture Radar) is a powerful energetic remote sensing technology that is used in a variety of applications, including flood monitoring. Radar is an active system that illuminates the Earth's surface, so images can be collected during the day under any lighting conditions, or at night in the complete absence of daylight. Furthermore, these images are unaffected by bad weather, fog, or smoke. As a result, radar signals can pass through these barriers [5, 6]. Continental waters, due to their low or no roughness in the absence of waves, behave like a mirror surface, reflecting the radar signal in the opposite direction of the sensor position, and thus exhibit very low backscatter values (negative) in comparison to other land covers. Because of the high contrast in backscatter values, SAR images can be used to precisely map flooded areas.

The importance of geospatial techniques in flood research cannot be overstated. It enables the proper integration of all physical, socioeconomic, and demographic data, as GIS's data management and map representation capabilities aid in the exploration of new areas. The combination of GIS and remote sensing improves the ability to forecast new scenarios and create flood hazard maps [7].

Many authors have used this methodology in other countries to perform flood monitoring and mapping [8]. However, within the region of the Niger Delta, the sentinel 1 image has not been used properly, and it has always been flooded for the past twenty years. This present study is an attempt to use sentinel 1 data to map flooded areas by comparing images acquired before and during the flood to distinguish flooded areas from permanent water bodies.

1.1. Geology and the Study Area

The area of study is within Yenagoa metropolis and its environs, which geologically is part of the Niger Delta sedimentary basin in Nigeria (Figure. 1). It lies within latitude $4^{o}57'30''N$-$4^{o}54'30''N$ and longitude $6^{o}15'30''E$-$6^{o}21'30''E$. The area has a well-developed road system that connects the constituent communities. The study area's topography ranges from 14.00 m to 38.00 m and is prone to flooding during the rainy season. Farming, fishing, and sand dredging from creeks and rivers are the main social and economic activities of the locals.

The Niger Delta is situated in the Gulf of Guinea on the West African Continental Margin. It has an area of approximately 105,000 square kilometers, occupying 60 percent of Nigeria's 800km of coastline and developing south-westwards out of the West African shield and west of the Oban Massif and the Tertiary Cameroon Volcanic Trend [9]. According to Doust and Omatsola [10], the Niger Delta has prograded south-westward, forming depobelts that represent the most active portion at each stage of its development. With an area of 300,000 sq. km, a sediment volume of 500,000 km3, and a sediment thickness of more than 10 km in the basin depocentre, these depobelts are among the world's largest regressive deltas.

Studies have revealed a tripartite lithostratigraphic succession, distinguished primarily by the sand-shale ratio [11]. The Benin Formation (an upper sand unit of continental origin), the Abgada Formation (an intervening unit of alternating sandstone and shale (paralic), and the Akata Formation are among the lithostratigraphic units (a lower shale unit of marine origin).

The Benin Formation is the most important aquiferous formation in this research area. At the basin's center, it's about 2100 meters thick. The quaternary deposits of the Benin Formation are about 40–120 m thick and composed of sand and silt, with the latter becoming more prominent seaward. Direct precipitation is the primary source of recharge, with annual rainfall reaching 3000mm [12]. Water infiltrates through the Benin Formation's highly permeable sands, replenishing the aquifers. Groundwater occurs primarily in the study areas under water table conditions.

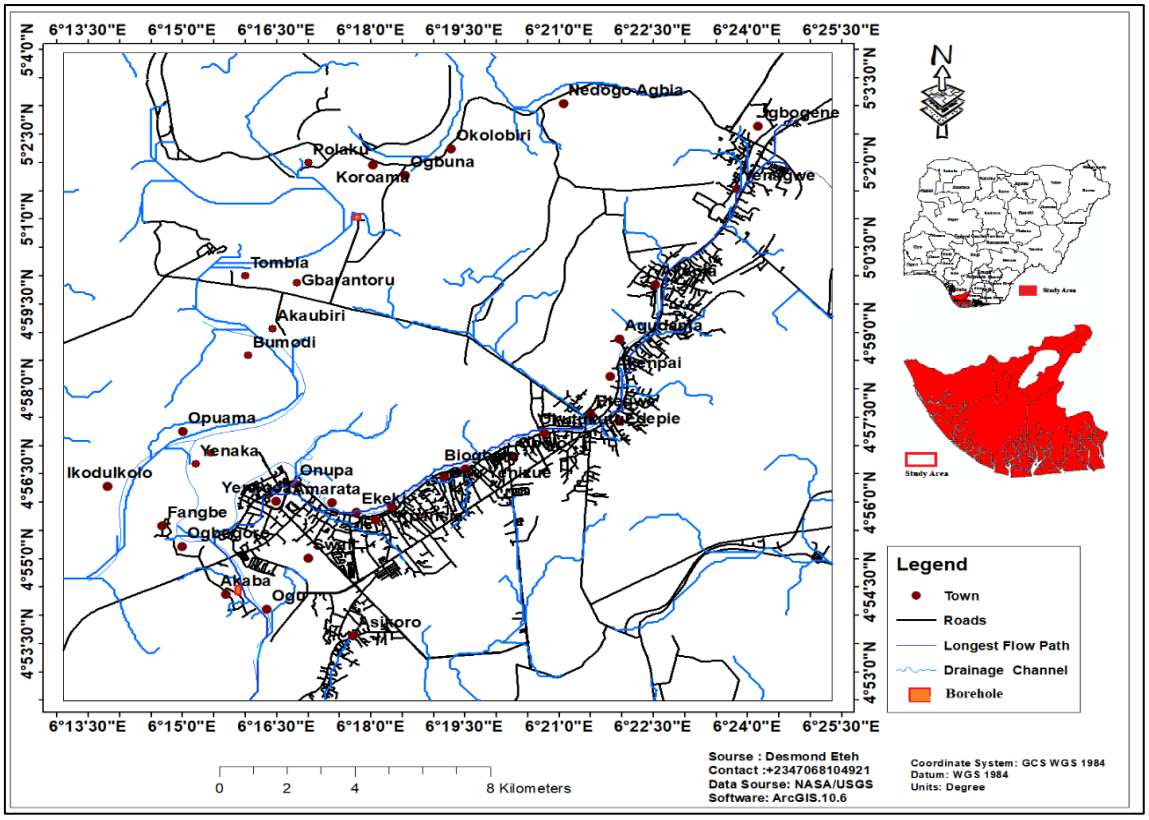

Figure-1. Study area map [7].

2. Materials and Method

2.1. Materials

Global Position System
Field notes

2.1.1. GIS and Remote Sensing Data Collection

Sentinel-1 SAR datasets for January, October, and November were obtained through the Copernicus Open Access Hub platform [13], as well as NASA's Google Earth Imagery (Table 1). The coordinates of the communities were obtained using the Garmin72 GPS device.

Table-1. List of data collected

Satellite Data	Date	Spatial Resolution	Source
Sentinel 1	Date: 01/31/2019 Path: 103 Frame :1196	10 m	[5]
Sentinel 1	Date: 17/10/2019 Path: 103 Frame :1196	10m	[5]
Sentinel 1	Date: 10/11/2019 Path: 103 Frame :572	10m	[5]
Google Earth Imagery	06/12/2019	3m	[14]

2.2. Methods

- Calibration threshold technique.

In accordance, the calibration threshold technique was used. It's a simple and quick process that generates histograms to distinguish flooded areas from those that aren't. This methodology is not advised for fast flash flooding, where visualization is required immediately and noise introduces ambiguity [15].

- RGB composition method

The RGB composition method is used to perform multi-temporal modifications and to detect changes on the terrain surface using a temporal colour image [16]. As a result, a multi-temporal image is created in which a band is assigned to each of the primary colours to form an RGB composition image [17].

2.2.1. Data Processing

2.2.1.1. Study Area Map Process

The Arc GIS software system in spatial analyst extension was used to generate the study area map by using the Global Positioning System (GPS) information and calculating it on Microsoft Excel and importing it into the Arc GIS environment in database format. The location map was generated alongside the digitizing of roads, rivers, and other properties.

2.2.1.2. SAR Sentinel-1 Processing

Lunch, the snap software 7.0.0 [18] system imports the image zone to pick a region of interest, subset, multi-look, calibrate, covert linear to/from decibel for higher image, and perform piece of land correction in alternative for geolocation of the image, applying contact stretch to the picked cell on each image to separate land from water, then layer stacking each image and applying RGB combination [17], or the detection or calibration threshold technique [19]. The methodologies used in this study were RGB composition and the calibrated thresholds technique. Before applying any techniques and performing multitemporal analysis, it is necessary to use a stack to unify the various bands of sima zero (σ0) of the images before and during the event into a single file.

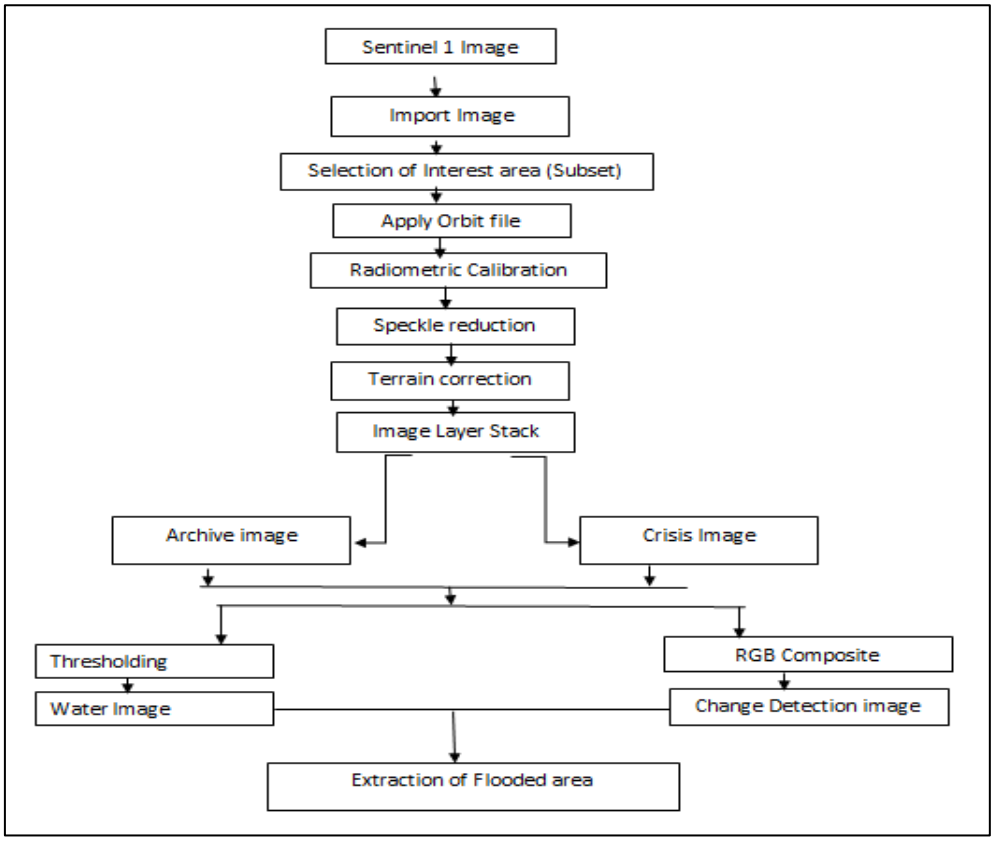

Figure-3.1. Flowchart for preprocessing chain used in Sentinel-1 images.

3. Results and Discussion

3.1. Results

The following result are provided for interpretation

Table-2. Statistical results of Sentinel 1 data for Archive and Disaster period

	19-Jan	19-Oct	19-Nov	Unit
Number of pixels total:	800172	800172	800172	
Number of considered pixels:	569320	517969	517969	
Ratio of considered pixels:	71.1497	64.7322	70.6172	%
Minimum:	-24.133	-24.584	-25.14	dB
Maximum:	23.6454	21.2582	20.1628	dB
Mean:	-7.6502	-7.8335	-7.9564	dB
Standard deviation:	3.24799	3.54012	3.5544	dB
Coefficient of variation:	-0.4273	-0.4519	-0.4467	dB
Median:	-7.3631	-7.4555	-7.5072	dB
P5 threshold:	-12.093	-15.462	-15.989	dB
P10 threshold:	-9.6087	-10.694	-10.96	dB
P15 threshold:	-9.0353	-9.5022	-9.6917	dB
P20 threshold:	-8.6531	-8.9979	-9.1027	dB

P25 threshold:	-8.3664	-8.6312	-8.695	dB
P30 threshold:	-8.1275	-8.3103	-8.4232	dB
P35 threshold:	-7.9364	-8.0811	-8.1514	dB
P40 threshold:	-7.7453	-7.8519	-7.9249	dB
P45 threshold:	-7.5542	-7.6685	-7.7436	dB
P50 threshold:	-7.3631	-7.4851	-7.5171	dB
P55 threshold:	-7.1719	-7.3017	-7.3359	dB
P60 threshold:	-6.9808	-7.0725	-7.1547	dB
P65 threshold:	-6.7897	-6.8892	-6.9282	dB
P70 threshold:	-6.5986	-6.66	-6.747	dB
P75 threshold:	-6.3597	-6.4307	-6.4752	dB
P80 threshold:	-6.1208	-6.1557	-6.2034	dB
P85 threshold:	-5.7864	-5.7889	-5.8409	dB
P90 threshold:	-5.2608	-5.193	-5.2973	dB
P95 threshold:	-4.0663	-3.5427	-3.8929	dB
Threshold max error:	0.04778	0.04584	0.0453	dB

4. Discussion

4.1. Calibration Threshold Technique

The magnitude of co-polarization (VV) intensity in the Niger Delta region of Yenagoa is highly variable, with a wide range of values for both the archive and disaster periods in October and November 2019. The areas adjacent to the river's course, which are mostly used for agriculture, have partially rough surfaces and moderate vegetation. Figures 3, 4, and 5 show the Value of Threshold for Land on the Histogram for the Co-polarization (VV) for January, October, and November 2019, which show different histograms with a smooth surface generated by the sheet of water. As a result, the backscatter intensity drops to even lower negative values, with high pick cells indicating land and low pick cells indicating water on the histogram.

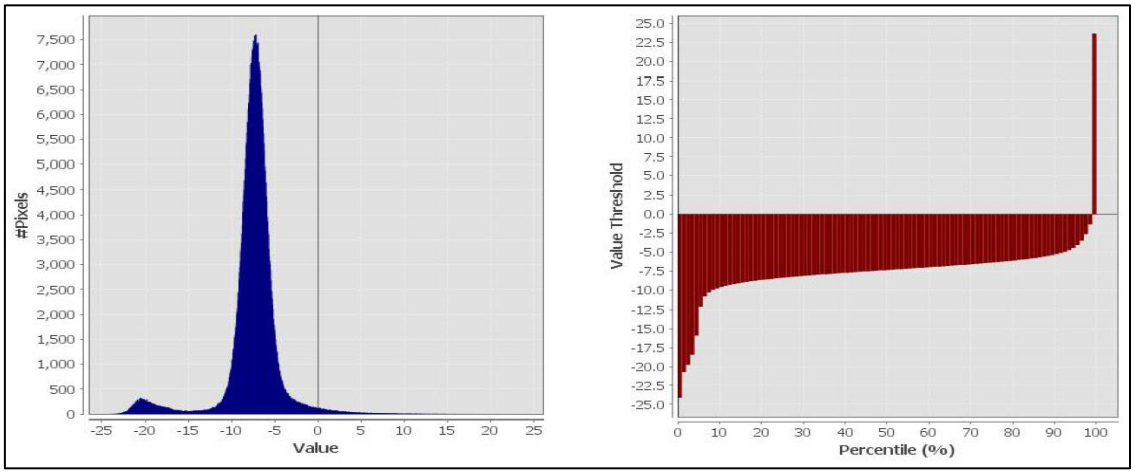

Figure-3. Characteristic histograms of Co-polarization (VV) in the Radar image of 7 January 2019 filtered with the Lee 3 × 3 window size filter

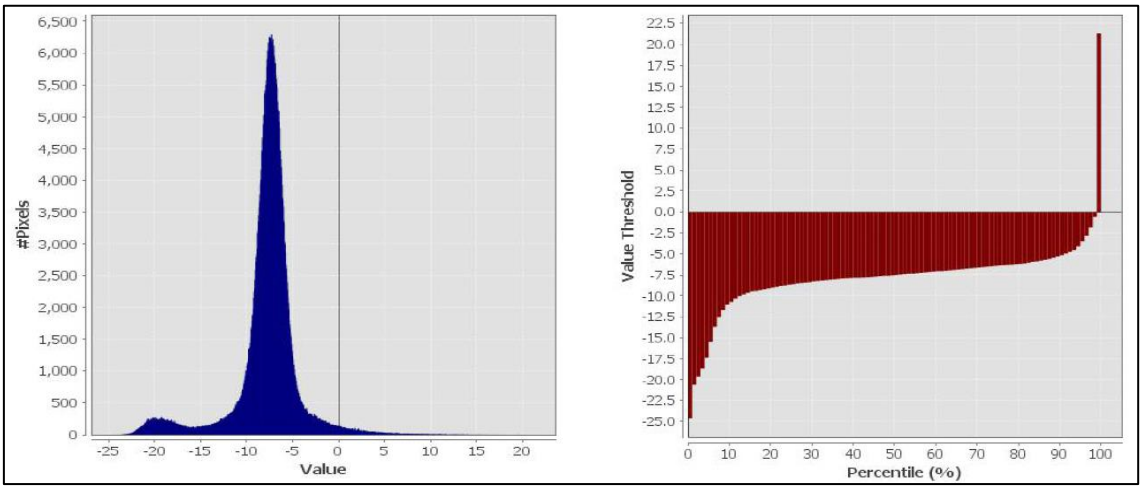

Figure-4. Characteristic histograms of Co-polarization (VV) in the Radar image of 17 October 2019 filtered with the Lee 3 × 3 window size filter

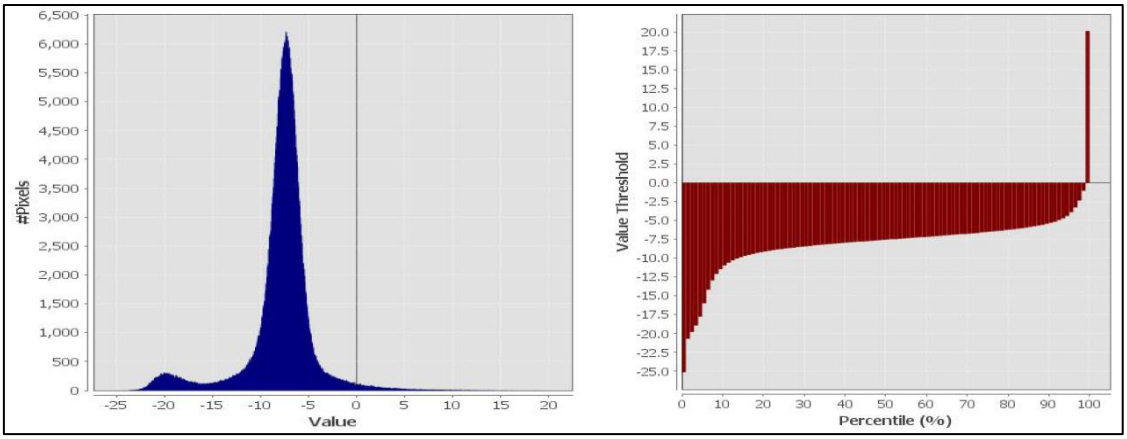

Figure-5. Characteristic histograms of Co-polarization (VV) in the Radar image of 11 November 2019 filtered with the Lee 3 × 3 window size filter

The graph shows the characteristics of the points. In Figure 6, we obtained an idea of the behavior of the radar on different surfaces. For the estimated mean water surface in Figure 6, the significant difference between January and October 2019 is -0.23 decibels (dB), while the difference between January and November 2019 is 0.36 dB, and the difference between October and November 2019 is -0.12 decibels (dB).The calibration threshold that separated the land from water bodies sheet through the interpretation of histograms in Figures 7 and 8 coupled with the relationship between polarization and characteristic histograms for each of them is observed in Figures 3, 4, and 5. The histogram for January 2019 of co-polarization (VV) shows a very large curve representative of the intensity values ranging between-24.13 and -23.64 dB. The histogram for October 2019 shows the minimum value of intensity values of-24.58 dB and maximum intensity values of -21.26 dB. It shows a range of intensity values from -25.14 to -20.16 dB for November 2019, indicating a very broad spectrum characteristic of areas ranging from very rough to moderately rough. Despite the fact that there is no clear projection of low backscatter values, this was chosen for further investigation. On the one hand, the curves in Figures 3, 4, and 5 provide more pixels than curves of smaller size and lower intensity values that represent water-filled areas, as shown in Table 2 and Figures 3, 4, and 5. The calibration limit can be set between each of these areas. When we examine the histograms in greater detail using contact stretch, we notice that cross-polarization provides a wider range of backscatter values on surfaces due to contact stretch on vegetation. co-polarization (VV), resulting in the omission of flooded areas in Figures 7 and 8.

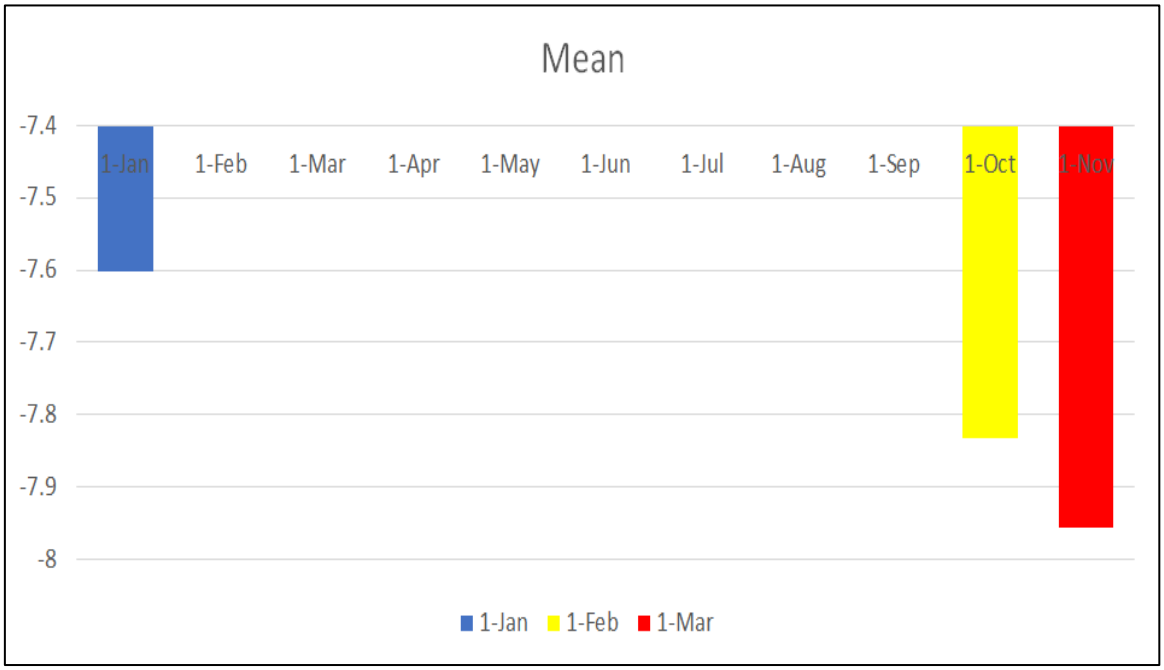

Figure-6. Intensity values of backscatter intensity before January 2019 and during the event for October and November 2019, for the Co-polarization (VV), for the indicated points

3.2.2. RGB Composition

To distinguish between the flooded area and permanent waterbodies, the RGB band technique was used (Figures 9 and 10). The image for the Archive and Crisis combined and the Red-band appears as red, which reflects the area with a high response on the red channel but a low response in the green and blue channels over the sounding area where we have no flood area, demonstrating the presence of grey tones as backscatter in Figures 6 and 7. Figures 7 and 8 show the different co-polarization (VV) results obtained in January, October, and November 2019. This combination reveals the visualization of the flooded areas, including water surfaces that are stable in Yenagoa.

Figures 9 and 10 show the populations of urban and industrial areas with very high-intensity values in white. As backscatter, areas with intermediate intensity values and few variations are unified into blue tones. The light pink tones are typical of humid areas, whereas the red depicts flood surfaces in Yenagoa, where the water has completely flooded. As a result, the flooding in the area is mostly fluvial flooding, which is caused by an excessive overflow of water, mostly rainwater, from the river into the surrounding environment and fills smaller streams, rivers, and lakes. This can be divided into two categories: flash flooding and overbank flooding [15]. The drainage system is responsible for the distribution pattern, and the area is revealed to be dendritic in nature [7].

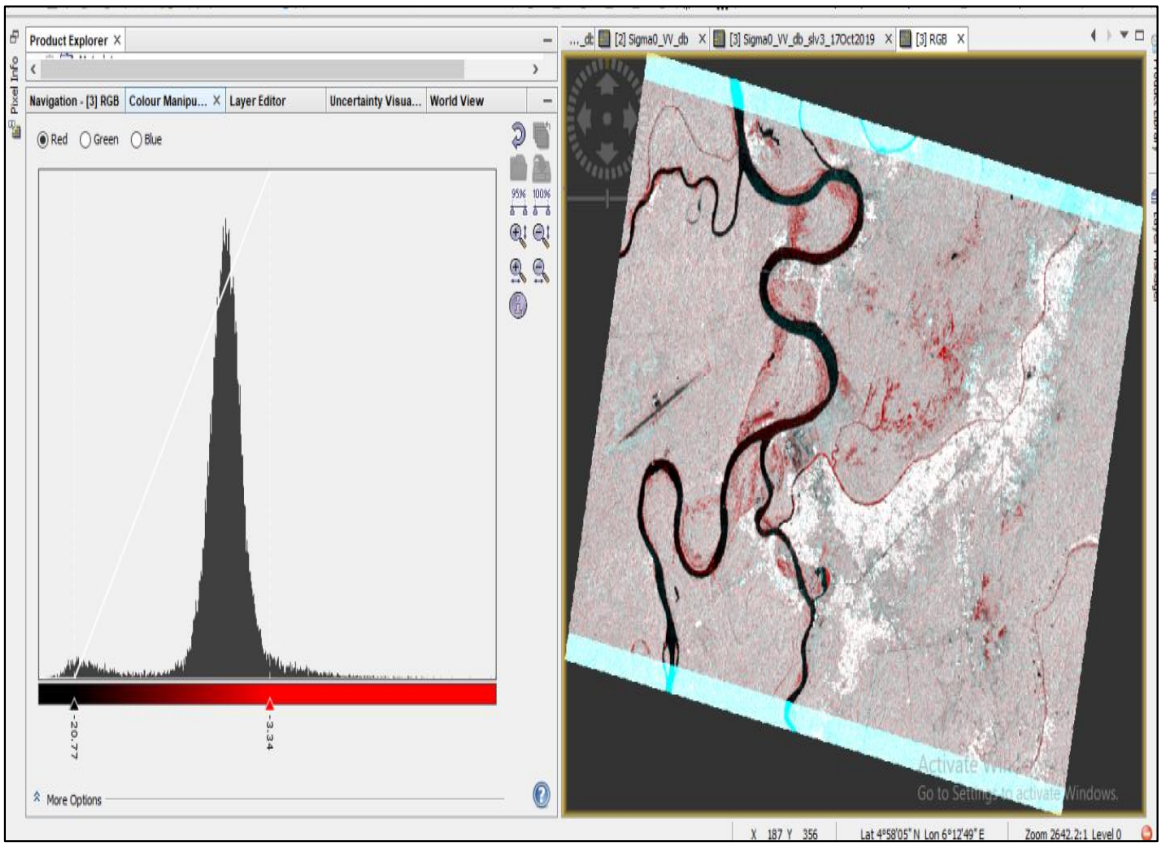

Figure-7. Characteristic histograms of Co-polarization (VV) in the Radar image for flooded area and land in October 2019

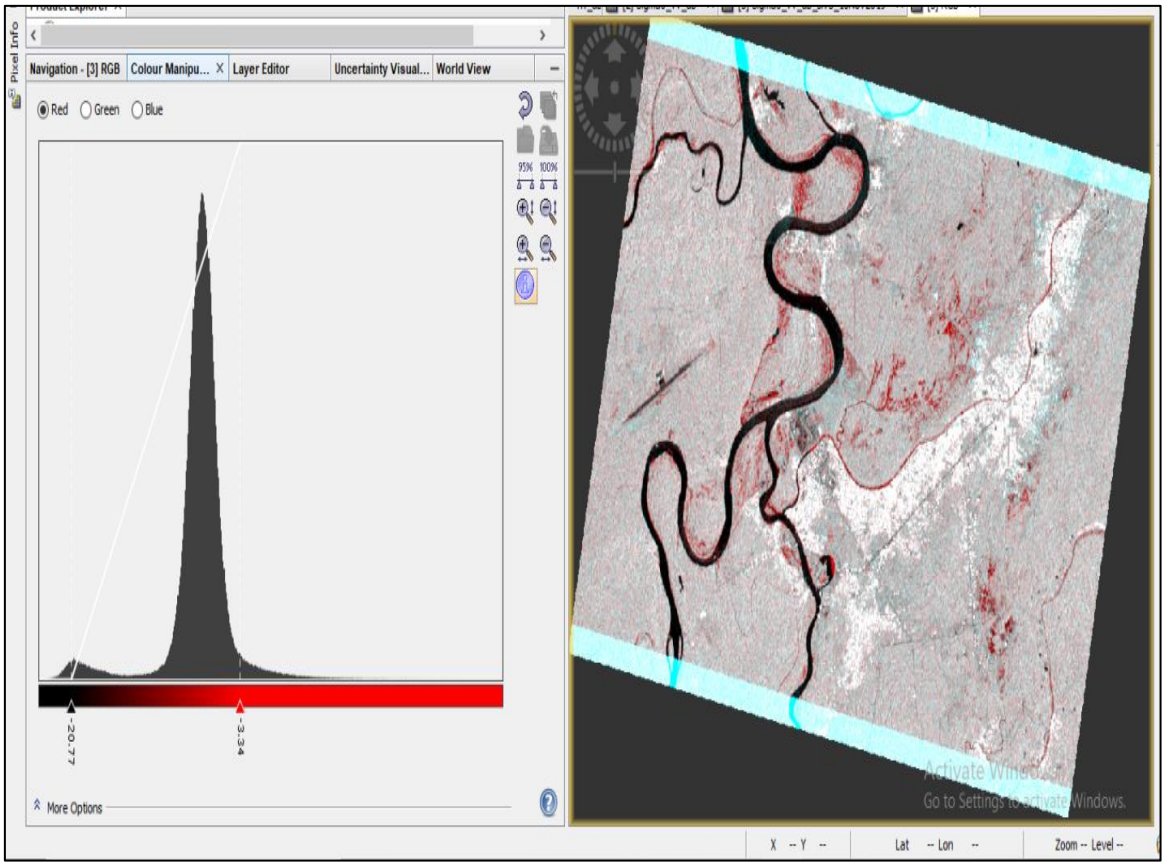

Figure-8. Characteristic histograms of Co-polarization (VV) in the Radar image for flooded area and land in November 2019

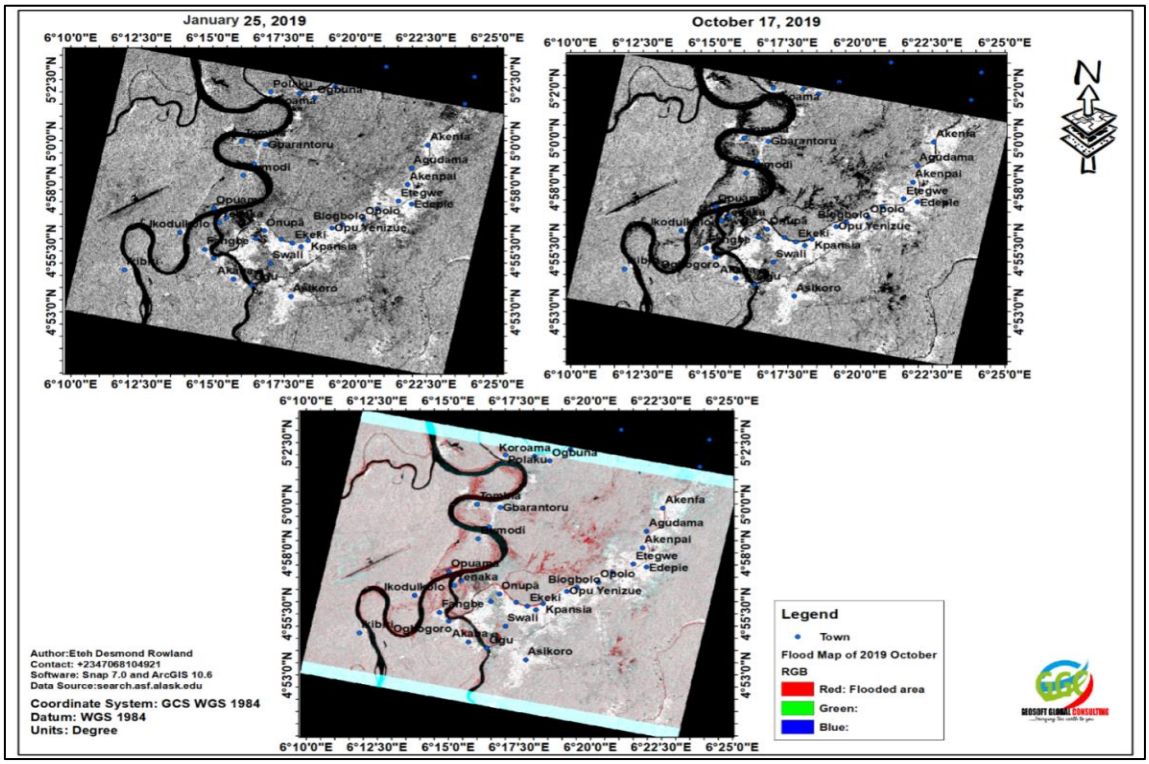

Figure-9. Flood map showing before the flood in January 2019 and during the event in October 2019, for the Co-polarization (VV), for the indicated points on the flooded area

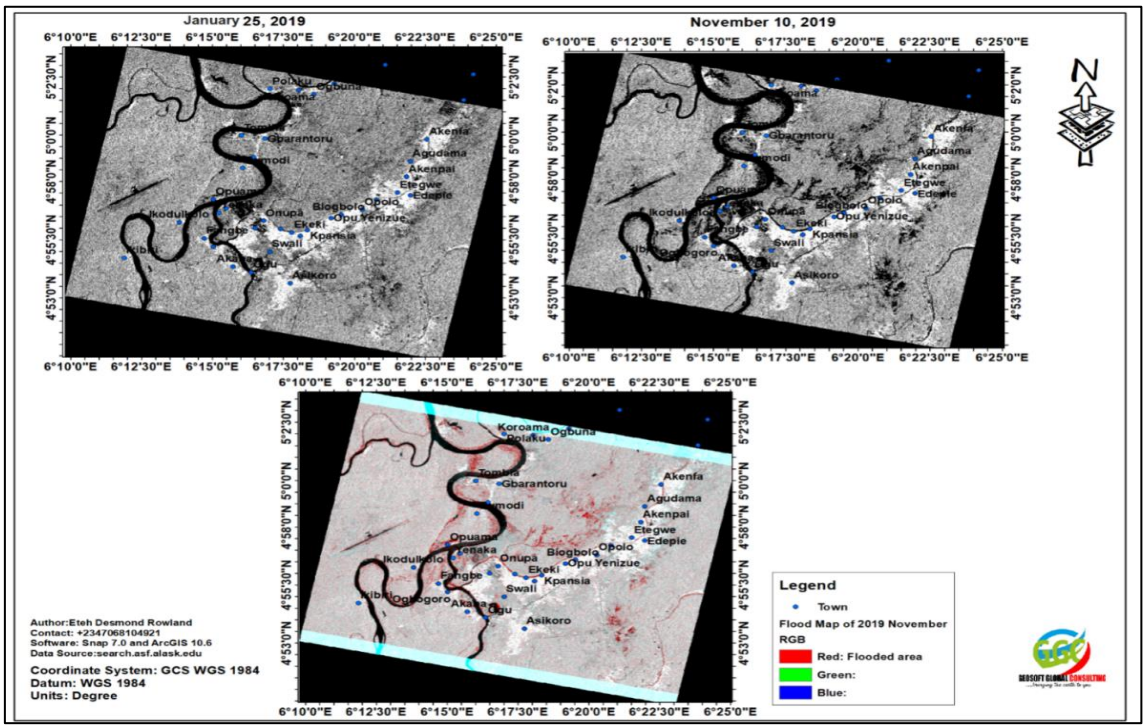

Figure-10. Flood map showing before the flood in January 2019 and during the event in November 2019, for the Co-polarization (VV), for the indicated points on the flooded area

5. Conclusions

The noble approach employs this technique for flood mapping and hazard observation in Yenagoa, Bayelsa State, using spatial resolution derived from Sentinel 1 images. Its specific goal was to map the potentially flooded area by utilizing Sentinel-1 data sets from the European Earth Observation mission for flood mapping and monitoring of hazards that occurred throughout the rainy season in Yenagoa.

By applying contact stretch to histograms, the applied techniques, RGB and Threshold, demonstrate a clear disparity between permanent water bodies and floods. Zones with low backscatter represent flooded areas in red, while zones with high radar response represent land in the archive. Permanent bodies of water are indicated by black, while built-up areas are indicated by white. The estimated significant difference in mean water surface for January and October 2019 is -0.23 decibels, while it is -0.36 decibels for January and November 2019. (dB). The estimated mean water surface in the study area differs by -0.12 decibels (dB) between October and November 2019.

The main advantage of using the RGB composition technique is that it ensures clear differentiation between areas of permanent flooding and those that are temporarily flooded, whereas achieving distinction using the calibration thresholds technique necessitates different processes.

Recommendation

Instead of rebuilding in a flood-ravaged area, why not turn it into a nature reserve for future disaster prevention; This will provide two benefits: recreation and water retention, which will help to prevent future flooding.

References

[1] Eteh, D. F., Emeka, E., and Francis, O., 2019. "Determination of flood hazard zones using geographical information systems and remote sensing techniques: A case study in part yenagoa metropolis." *Journal of Geography Environment and Earth Science International*, vol. 21, pp. 1-9.

[2] The United Nations Office for Disaster Risk Reduction UNISDR, 2015. "The Human Cost of Weather Related Studies. 2015." Available: https://www.unisdr.org/2015/docs/climatechange/COP21_WeatherDisastersReport_2015_FINAL.pdf

[3] European Environment Agency, 2016. *Flood Risks and Environmental Vulnerability; Exploring the Synergies between Floodplain Restoration, Water Policies and Thematic Policies; European Environment Agency*. Copenhagen, Danmark, pp. 9–15.

[4] Usoro, U. E., 2004. *Assessment and Mitigation Strategies of Flood Risk. In Akwa Ibom State A Geographical Perspective*. London: Enugu.

[5] Copernicus Open Access Hub, 2019. Available: https://scihub.copernicus.eu/(accessed

[6] Cunjian, Y., Yiming, W., Siyuan, W., Zengxiang, Z., and Shifeng, H., 2001. "Extracting the flood extent from satellite SAR image with thesupport of topographic data." In *Proceedings of the International Conferences on Info-Tech and Info-Net. Networks (ICII 2001), Beijing, China, 29 October–1 November 2001; IEEE: Piscataway, NJ, USA.* pp. 87–92.

[7] Eteh, D. R. and Akana, T. S., 2020. "Flood simulation and Terrain Analysis between 2018 and 2019 in the Niger Delta: A case study of Yenagoa and its environs." *International Research Journal of Modernization in Engineering Technology and Science*, vol. 2.

[8] Francisco, C. C. and Marita, D. M., 2019. "Flood Monitoring Based on the Study of Sentinel-1 SAR Images." *The Ebro River Case Study Water*, vol. 11, p. 2454. Available: https://doi.org/10.3390/w11122454

[9] Reijers, T. J. A., 2011. "Stratigraphy and Sedimentology of the Niger Delta." *Geologos TheNetherlands*, vol. 17, pp. 133-162.

[10] Doust, H. and Omatsola, E., 1990. *Niger delta, in, edwards, j. D., and santogrossi, p.A., eds., divergent/passive margin basins, aapg memoir 48*. Tulsa: American Association of Petroleum Geologists. pp. 239-248.

[11] Short, K. C. and Stauble, A. J., 1967. "Outline of the Geology of the Niger Delta." *AAPG Bulletin*, vol. 51, pp. 761-779.

[12] Amajor, L. C. and Ofoegbu, C. O., 1988. "Determination of Polluted Aquifers by Stratigraphically Controlled Biochemical Mapping; Eastern Niger Delta, Nigeria", Groundwater and Mineral Resources of Nigeria." pp. 62-73.

[13] European Space Agency ESA, 2019. "The ASAR user guide." Available: https://earth.esa.int/handbooks/asar/toc.html

[14] Available: http://www.google.com/earth/

[15] Westerhoff, R. S., Kleuskens, M. P. H., Winsemius, H. C., Huizinga, H. J., Brakenridge, G. R., and Bishop, C., 2013. "Automated global water mapping based on wide-swath orbital synthetic-aperture Radar." *Hydrol. Earth Syst. Sci.*, vol. 17, pp. 651–663.

[16] Amitrano, D., Guida, R., and Ruello, G., 2019. "Multitemporal sar rgb processing for sentinel-1 grd products: Methodology and applications." *IEEE J. Select. Top. Appl. Earth Obs. Remote Sens*, vol. 12, pp. 1497–1507.

[17] Tavus, B., Kocaman, S., Gokceoglu, C., and Nefeslioglu, H. A., 2018. "Considerations on the use of sentinel-1 data in flood mapping in urban areas: Ankara (turkey) 2018 floods. Int. Arch. Photogramm. ." *Remote Sens. Spat. Inf. Sci.*, vol. XLI, pp. 575-581.

[18] SNAP Software Version 7.0.0, 2019. Available: https://step.esa.int/main/download/snap-download

[19] Martinis, S. and Rieke, C., 2015. "Backscatter analysis using multi-temporal and multi-frequency SAR data in the context of flood mapping at river Saale, Germany." *Remote Sensing*, vol. 7, pp. 7732–7752.